Supplementary Information

Environmental precursors to rapid light carbon injection at the Palaeocene/Eocene boundary

Appy Sluijs, Henk Brinkhuis, Stefan Schouten, Steven M. Bohaty, Cédric M. John, James C. Zachos, Gert-Jan Reichart, Jaap S. Sinninghe Damsté, Erica M. Crouch, Gerald R. Dickens

This section contains four figures and additional references. Figures S1 and S2 comprise the complete records of the New Jersey sites Bass River and Wilson Lake, respectively. Figure S3 includes data that shows that the onset of the *Apectodinium* acme also occurred prior to the carbon isotope excursion (CIE) in the North Sea and the southwest Pacific Ocean. Potential precession forcing on the dinocyst records at Bass River is discussed (Figure S4). Finally, we discuss the cause of the *Apectodinium* acme and planktonic foraminifer $\delta^{18}O$ data.

Organic hypnozygotic dinoflagellate cysts (dinocysts)

Dinoflagellates are single-celled, predominantly marine, eukaryotic plankton that typically occur as motile cells in surface waters[1,2]. As part of their life cycle, some dinoflagellates produce organic (hypnozygotic) resting cysts (dinocysts). This dormant or 'cyst' part of the dinoflagellate life cycle is related to sexual reproduction. Cyst formation is induced by particular surface water parameters, usually nutrient depletion following a bloom[1]. Typically, the motile stage does not preserve, but organic dinocysts are very resistant to oxidation and are found from the Late Triassic onwards[3]. Records from the deep sea are rare, primarily because oxidation hampers their preservation in such environments, so they are mostly found in siliciclastic sediments deposited on the shelf or slope.

Derivation of maps in Figure 1.

The maps that represent the left and right panel in Figure 1 are modified from refs. 4 and 5, respectively.

Potential precession forcing on *Apectodinium* abundance at Bass River

Estimates for the duration of the CIE range between 130 kyr and 220 kyr[6,7] but was likely close to 170 kyr[8-10]. Accepting this number gives sedimentation rates through the 10.3 meter thick CIE at Bass River (Fig. S1) of ~6.1 $cm.kyr^{-1}$. However, the upper bound of the CIE in this section is represented by a (sea level) sequence boundary[11,12], which implies that the upper part of the CIE is not represented here. Omitting this truncation skews sedimentation rate estimates across the CIE towards lower values. However, we speculate that the 5 or 6 cyclic fluctuations in the relative and absolute abundance records of *Apectodinium* and the number of dinocysts per gram of sediment could be related to climatic forcing in the precession band (Fig. S4). Ecologically, this would imply that neritic surface water parameters (likely salinity, since the abundance of low-salinity tolerant taxa varies in anti-phase with the *Apectodinium* abundance; Fig. S4) varied as a result of precession forcing, which has been recorded many times in dinocyst records from neritic Eocene deposits[13,14]. Five cycles are present in the record, but considering that the lower one is associated with transgressive systems tract and thus likely with slightly lower sedimentation rates[12] (Fig. S4) this may actually represent two precession cycles. However, the lower one of these two predates the CIE, so 5 cycles are present within the CIE. Five cycles would imply that ~100 kyr of PETM section is present at Bass River, resulting in average sedimentation rates of ~10 $cm.kyr^{-1}$ within the PETM.

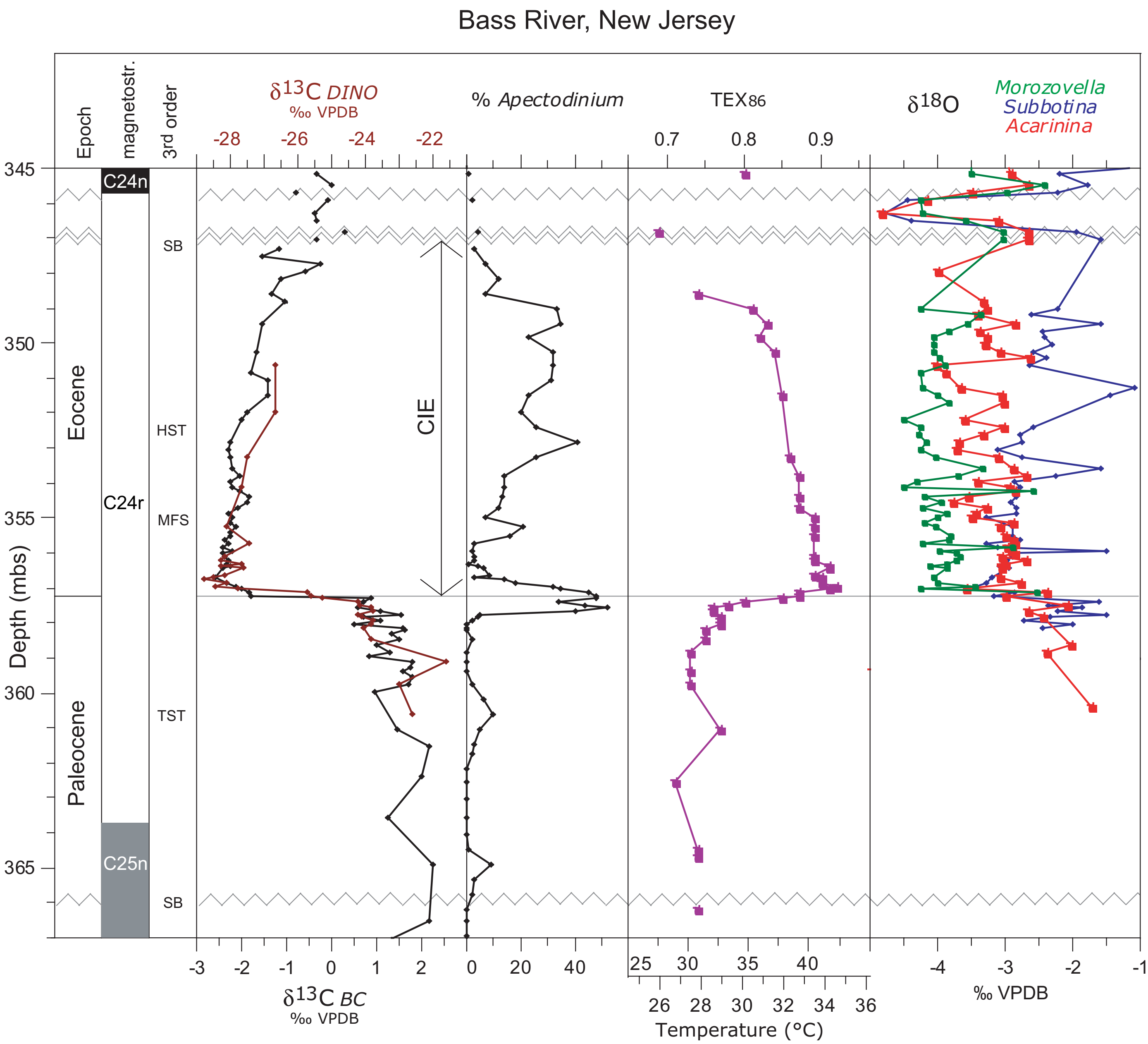

Figure S1. High-resolution records across the entire PETM interval at Bass River, New Jersey. Figure 2a in the main text represents a zoom of this record across the onset of the CIE. Solid horizontal line at ~357.3 mbs represents the onset of the CIE. BC = bulk carbonate, DINO = dinocysts, VPDB = Vienna Pee Dee Belemnite, mbs = meters below surface. Zigzag lines represent sequence boundaries, adapted from refs. 11, 12. Scales at TEX86 temperatures represent calibrations from ref. 24 for the top bar and from ref. 25 for the lower bar. Stable oxygen isotope data on foraminifera are from ref. 23.

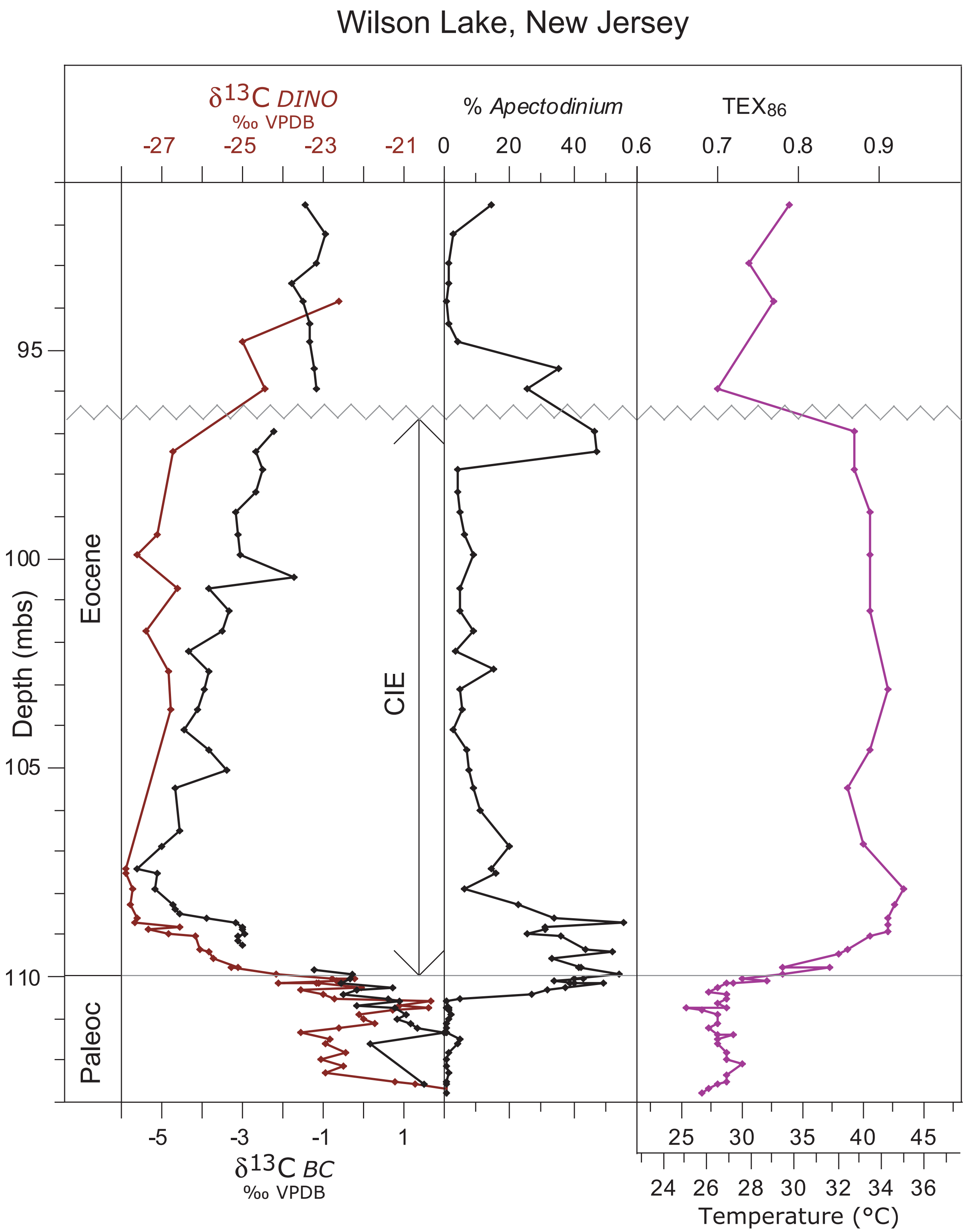

Figure S2. High-resolution records across the PETM at Wilson Lake, New Jersey. Figure 2b in the main text represents a zoom of this record across the onset of the CIE. Solid horizontal line at ~110.0 mbs represents the onset of the CIE. Zigzag lines represent sequence boundaries, adapted from refs. 12, 22, 26. BC = bulk carbonate, DINO = dinocysts, VPDB = Vienna Pee Dee Belemnite, mbs = meters below surface. TEX_{86} data partially from ref. 22 (see Table S1 for details).

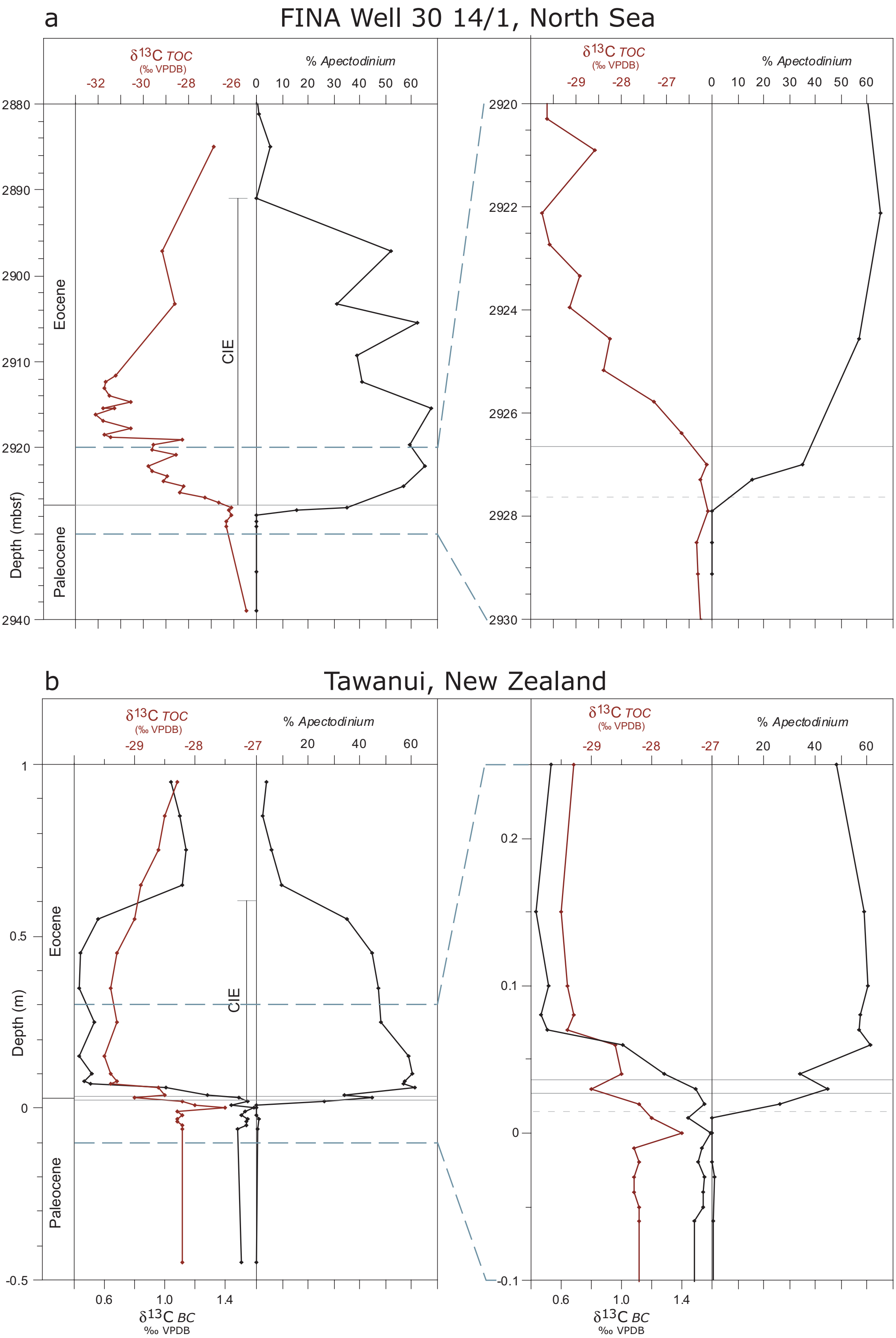

Figure S3. FINA Well 30 14/1, North Sea (**a**) and Tawanui, New Zealand (**b**). Tawanui data are from refs. 16, 17. Left panels represent the entire PETM records, right panels show an enlarged view on the intervals around the onset of the CIE. Solid lines indicate the onset of the CIE (two options for Tawanui), while dashed lines mark the onset of the *Apectodinium* acme. DINO = dinocysts, TOC = Total Organic Carbon, VPDB = Vienna Pee Dee Belemnite, mbs = meters below surface, mbsf = meters below sea floor.

The *Apectodinium* acme and the CIE in the North Sea and southwest Pacific

We also studied industry well FINA 30/14-1, from the central North Sea at ~55 °N palaeolatitude (Fig. 1). At this central North Sea site, we identified the PETM based on the occurrence of a negative CIE in $\delta^{13}C$ records of total organic carbon ($\delta^{13}C_{TOC}$) (Fig. S3), and by the presence of the dinoflagellate species *Apectodinium augustum*, which is diagnostic of the PETM[15]. The CIE is ~37 m thick at this site (Fig. S3). The onset of the CIE is at ~2926.7 meters below sea floor (mbsf) and its termination approximately 37 meters higher (Fig. S3). Given a duration of 170 kyr for the CIE[8-10], average sedimentation rate at this site were ~22 cm.kyr^{-1}. The onset of the *Apectodinium* acme is 80 cm below the onset of the CIE at ~2927.5 mbsf, implying that also at this site the onset of the acme again leads the CIE by about 4 kyr. Notably, this site is located in the central North Sea, so sedimentation rates were presumably fairly constant near the start of the PETM. TEX_{86} palaeothermometry is not possible on the sediments from the North Sea section; the crenarchaeotal membrane lipids are not present because of the relatively high maturity of the organic matter.

Although less obvious, this sequence of events is supported by the records from the condensed Tawanui section in New Zealand, deposited in upper bathyal water depths at ~55°S palaeolatitude in the southwest Pacific Ocean[16, 17] (Fig. 1). The onset of the CIE in this section is somewhat ambiguous: typical latest Palaeocene values in the $\delta^{13}C_{BC}$ record occur up to 0.04 m (Fig. S3), but background values in the $\delta^{13}C_{TOC}$ record are present up to 0.03 m. Above this level, the CIE starts. The onset of the *Apectodinium* acme is at 0.02 m and, hence, below the CIE (Fig. S3). Calculation of the time lag involved is complicated by the condensed nature of this section.

The causes of the global *Apectodinium* acme

Identification of the environmental parameters that caused the *Apectodinium* acme is vital in understanding the sequence of climatological events that eventually caused the warming and the CIE. Crouch et al. (ref. 18, p. 125) note that any *Apectodinium* bloom required "a special set of environmental conditions" of which a baseline requirement appears to be high temperatures. *Apectodinium* acmes have been recorded from upper Palaeocene deposits in the Tethyan Ocean[19], suggesting that conditions there were episodically and locally similar to those on a global scale during the PETM[18]. Similar to other mid-latitude regions, *Apectodinium* was already present on the New Jersey shelf at least since Chron C25n (Fig. S1); yet, in contrast to low-latitude sites[19] no pre-PETM acmes have been reported from such regions. Since *Apectodinium* was abundant in the Arctic Ocean with SSTs around 23 °C (ref. 20), New Jersey shelf SSTs during the late Palaeocene should have already been high enough to allow for abundant *Apectodinium*. This implies that some other environmental parameter(s) prevented the establishment of late Palaeocene *Apectodinium* acmes in the mid latitudes.

It has been noted that *Apectodinium* locally became outnumbered by typical low-salinity tolerant dinocysts during the PETM[20]. This observation is consistent with the records from the New Jersey shelf (Fig. S4), indicating that very low salinities were not optimal for *Apectodinium*. Other proposed ecological requirements include stratified surface waters[18]. Moreover *Apectodinium* has morphological characteristics identical to cysts of modern heterotrophic dinoflagellates, which has fueled the hypothesis that *Apectodinium* was a heterotrophic dinoflagellate[15]. Basic predator-prey abundance models indicate that with higher nutrient supplies, ecosystems should become relatively enriched in organisms that are higher up in the food chain, i.e., heterotrophic. The total amount of dinoflagellate cysts per gram of sediment, which reflects cyst production and thereby nutrient supply during the PETM at Bass River, co-varies with the absolute abundance of *Apectodinium* cysts (Fig. S4). This suggests that higher nutrient levels are directly reflected in higher production of *Apectodinium* cysts, supporting the hypothesis that *Apectodinium* was a heterotrophic dinoflagellate. Increasing nutrient levels may, therefore, have contributed to the *Apectodinium* acme. If so, the global character of the acme implies that at least neritic sections underwent significant eutrophication on a global scale[15, 16], a hypothesis corroborated by many proxy data (see overview in ref. 10). Modern dinoflagellate blooms usually last for several days to weeks[21]. Conceivably, *Apectodinium* blooms during the PETM had similar dynamics, in which case the pre-CIE signal would imply a change in specific seasonal conditions of the surface waters. This may include any of the above environmental factors. However, even a combination of these factors was likely not truly unique in the early Palaeogene, suggesting that some critical environmental factor has not yet been identified. Whichever combination of surface water parameters caused the global acme of *Apectodinium*, it is consistently associated with the PETM and appears to signify a harbinger to global warming and carbon injection.

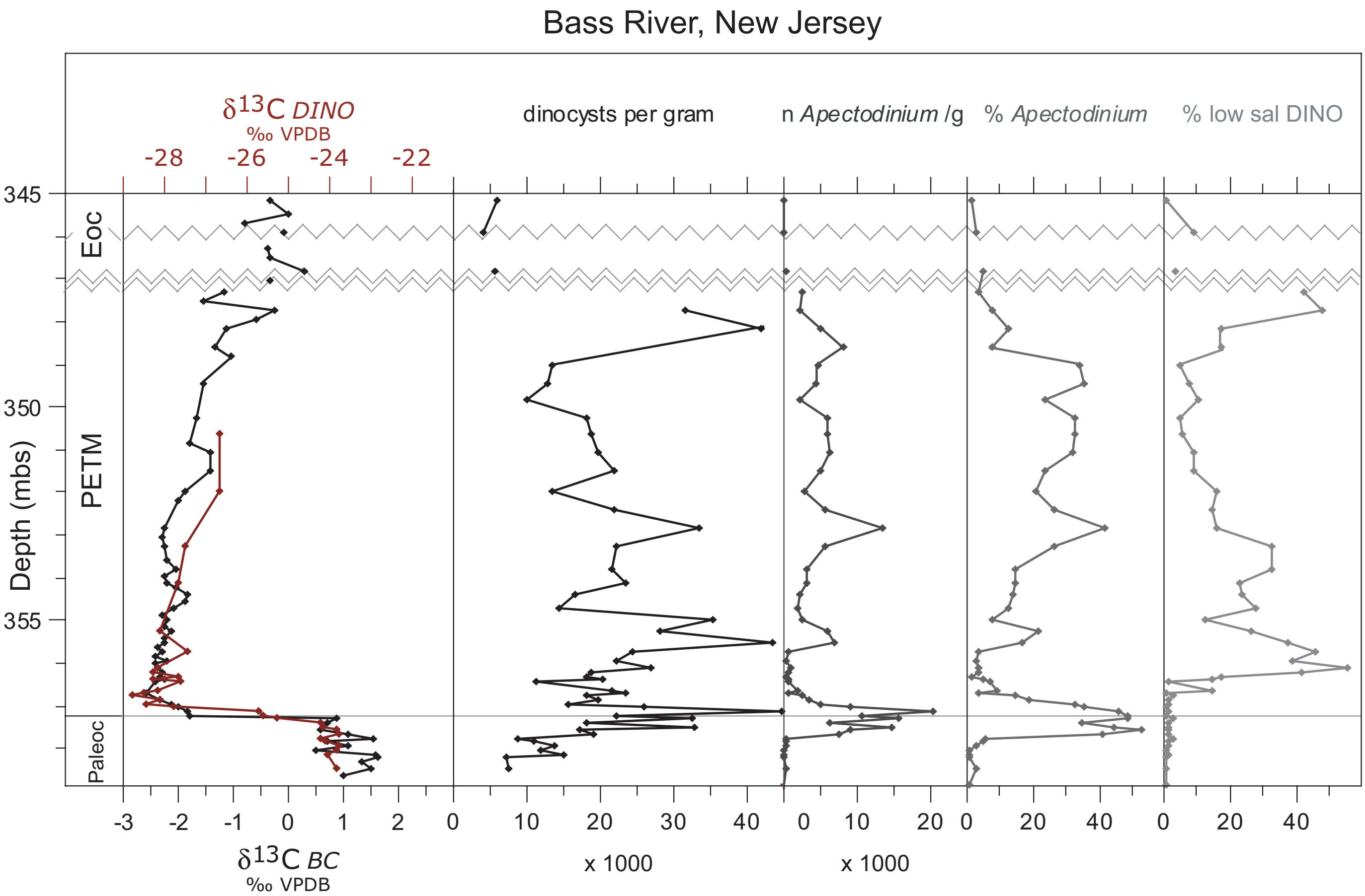

Figure S4. High-resolution dinocyst records across the PETM at Bass River. See pages 1 and 5 for discussion. Bulk carbonate stable isotope data from ref. 23. BC = bulk carbonate, DINO = dinocysts, low sal = low salinity tolerant, VPDB = Vienna Pee Dee Belemnite, mbs = meters below surface.

New Jersey planktonic foraminifer ^{18}O records

At Bass River and Wilson Lake, surface dwelling foraminifer δ^{18}O data have been generated[22, 23]. At Bass River, the negative δ^{18}O excursions in the surface dwellers *Acaranina* (~-0.6‰) and *Morozovella* (~-0.9‰) are rather small and imply only ~3 °C warming of surface waters, assuming no change in salinity[23]. However, the Bass River and Wilson Lake TEX_{86} records and the Wilson Lake planktonic foraminifer δ^{18}O record consistently point to 7-9 °C of surface ocean warming on the New Jersey Shelf. These issues indicate that factors other than temperature, such as variations in seawater δ^{18}O and diagenesis, influenced the planktonic foraminifer δ^{18}O record at Bass River. Moreover, single shell δ^{18}O values from individual samples show a large spread (~1‰)[23], with standard deviations of ~0.5‰. Such a spread is common in modern populations of planktonic foraminifera but this alone implies 2 °C uncertainty in the δ^{18}O-derived relative temperature estimates. Because of the large scatter and high standard deviations from single shell analyses, within and between samples, it is hard to pinpoint the stratigraphic level at which the values start to decrease. Critically, no foraminifera suitable for δ^{18}O analysis were present in the sample at 357.30 mbs, just below the onset of the CIE, potentially due to dissolution.

At Wilson Lake, only few planktonic foraminifera suitable for δ^{18}O analyses are present below the CIE[22]. These values are 1.5 – 2‰ higher than PETM values, evidencing that the magnitude of sea surface warming at Wilson Lake comprised ~6-8 °C during the PETM[22]. However, due to the scarcity of data below the CIE, the stratigraphic level at which foraminifer δ^{18}O values start to decrease is unclear.

Supplementary References

1. Taylor, F. J. R. (ed.) The biology of dinoflagellates (Blackwell Scientific Publications, London, 1987).
2. Fensome, R. A., Gocht, H. & Williams, G. L. The Eisenack Catalog of Fossil Dinoflagellates. New Series. Volume **4** (E. Schweizerbart'sche Verlagsbuchhandlung, Stuttgart, Germany, 1996).
3. MacRae, R. A., Fensome, R. A. & Williams, G. L. Fossil dinoflagellate diversity, originations, and extinctions and their significance. Canadian Journal of Botany **74**, 1687-1694 (1996).
4. Miller, K. G. in Proceedings of the Ocean Drilling Program, Scientific Results, Volume 150X (eds. Miller, K. G. & Snyder, S. W.) 3–12 (Ocean Drilling Program, College Station, TX, 1997).
5. Scotese, C. P. & Golanka, J. Paleogeographic atlas, PALEOMAP progress report 20-0692 (University of Texas, Arlington, 1992).
6. Farley, K. A. & Eltgroth, S. F. An alternative age model for the Paleocene-Eocene thermal maximum using extraterrestrial ^{3}He. Earth and Planetary Science Letters **208**, 135-148 (2003).
7. Röhl, U., Bralower, T. J., Norris, G. & Wefer, G. A new chronology for the late Paleocene thermal maximum and its environmental implications. Geology **28**, 927-930 (2000).
8. Röhl, U., Westerhold, T., Bralower, T. J. & Zachos, J. C. in Climate and Biota of the Early Paleogene (CBEP2006). 112 (Bilbao, Spain, 2006).
9. Abdul Aziz, H., Gingerich, P. D., Hilgen, F. J., van Luijk, G. & Sluijs, A. in Climate and Biota of the Early Paleogene (CBEP2006). 1 (Bilbao, Spain, 2006).
10. Sluijs, A., Bowen, G. J., Brinkhuis, H., Lourens, L. J. & Thomas, E. in Deep time perspectives on Climate Change (eds. Williams, M., Haywood, A., Gregory, J. & Schmidt, D. N.) (Geological Society of London, TMS Special Publication, London, in press, November 2007).
11. Cramer, B. S. et al. An exceptional chronologic, isotopic, and clay mineralogic record of the latest Paleocene thermal maximum, Bass River, NJ, ODP 174AX. Bulletin de la Société Géologique de France **170**, 883-897 (1999).
12. Sluijs, A. Global Change during the Paleocene-Eocene thermal maximum (Laboratory of Palaeobotany and Palynology Foundation No. 21, Utrecht, The Netherlands, 2006).
13. Röhl, U. et al. in The Cenozoic Southern Ocean: Tectonics, Sedimentation, and Climate Change Between Australia and Antarctica. American Geophysical Union Geophysical Monograph Series, 151 (eds. Exon, N. F., Malone, M. & Kennett, J. P.) 127-151 (2004).
14. Warnaar, J. Climatological Implications of Australian-Antarctic Separation (Laboratory of Palaeobotany and Palynology Foundation No. 22, Utrecht, The Netherlands, 2006).
15. Bujak, J. P. & Brinkhuis, H. in Late Paleocene - early Eocene climatic and biotic events in the marine and terrestrial records (eds. Aubry, M.-P., Lucas, S. G. & Berggren, W. A.) 277-295 (Columbia University Press, New York, 1998).
16. Crouch, E. M. et al. Global dinoflagellate event associated with the late Paleocene thermal maximum. Geology **29**, 315-318 (2001).
17. Crouch, E. M. et al. The *Apectodinium* acme and terrestrial discharge during the Paleocene-Eocene thermal maximum: new palynological, geochemical and calcareous nannoplankton observations at Tawanui, New Zealand. Palaeogeography, Palaeoclimatology, Palaeoecology **194**, 387-403 (2003).
18. Crouch, E. M., Brinkhuis, H., Visscher, H., Adatte, T. & Bolle, M.-P. in Causes and Consequences of Globally Warm Climates in the Early Paleogene. Geological Society of America Special Paper 369 (eds. Wing, S. L., Gingerich, P. D., Schmitz, B. & Thomas, E.) 113-131 (Geological Society of America, Boulder, Colorado, 2003).
19. Iakovleva, A. I., Brinkhuis, H. & Cavagnetto, C. Late Palaeocene-Early Eocene dinoflagellate cysts from the Turgay Strait, Kazakhstan; correlations across ancient seaways. Palaeogeography, Palaeoclimatology, Palaeoecology **172**, 243-268 (2001).
20. Sluijs, A. et al. Subtropical Arctic Ocean temperatures during the Palaeocene/Eocene thermal maximum. Nature **441**, 610-613 (2006).
21. Dale, B. in Palynology: Principles and Applications (eds. Jansonius, J. & McGregor, D. C.) 1249-1276 (American Association of Stratigraphic Palynologists Foundation, Dallas, 1996).
22. Zachos, J. C. et al. Extreme warming of mid-latitude coastal ocean during the Paleocene-Eocene Thermal Maximum: Inferences from TEX_{86} and Isotope Data. Geology **34**, 737-740 (2006).
23. Zachos, J. C. et al. The Palaeocene-Eocene carbon isotope excursion: constraints from individual shell planktonic foraminifer records. Philosophical Transactions of the Royal Society A **365**, 1829-1842 (2007).
24. Schouten, S., Hopmans, E. C., Schefuß, E. & Sinninghe Damsté, J. S. Distributional variations in marine crenarchaeotal membrane lipids: a new tool for reconstructing ancient sea water temperatures? Earth and Planetary Science Letters **204**, 265-274 (2002).
25. Schouten, S. et al. Extremely high sea-surface temperatures at low latitudes during the middle Cretaceous as revealed by archaeal membrane lipids. Geology **31**, 1069-1072 (2003).
26. Gibbs, S. J., Bralower, T. J., Bown, P. R., Zachos, J. C. & Bybell, L. M. Shelf and open-ocean calcareous phytoplankton assemblages across the Paleocene-Eocene Thermal Maximum: Implications for global productivity gradients. Geology **34**, 233-236 (2006).

Table S1 (next page). Palynological, TEX_{86} and isotope data of sites **a.** Bass River, **b.** Wilson Lake and **c.** North Sea.

Table 1a. Bass River

Bass River Dinocyst assemblage data

top (feet)	top (tenth of feet)	bottom (feet)	bottom (tenth of feet)	top (mbs)	bottom (mbs)	Av depth (mbs)	% *Apectodinium*	% low salinity tolerant dinocysts	n *Apectodinium* / g sediment	n low salinity tolerant dinocysts / g sediment
1132	4	1132	5	345.16	345.19	345.17	1	0	77	26
1134	9	1135	0	345.92	345.95	345.93	2	9	61	333
1137	8	1137	9	346.80	346.83	346.82	4	3	207	145
1139	4	1139	5	347.29	347.32	347.30	3	43	2471	36185
1140	8	1140	9	347.72	347.75	347.73	7	51	2189	14869
1142	3	1142	4	348.17	348.20	348.19	12	19	4929	7159
1143	7	1143	8	348.60	348.63	348.62	7	18	8127	19810
1145	1	1145	2	349.03	349.06	349.04	33	5	4534	488
1146	4	1146	5	349.42	349.45	349.44	35	10	4409	855
1147	7	1147	8	349.82	349.85	349.83	23	13	2266	977
1149	1	1149	2	350.25	350.28	350.26	32	6	5914	749
1150	4	1150	5	350.64	350.67	350.66	32	8	5888	981
1151	8	1151	9	351.07	351.10	351.08	31	11	6123	1498
1153	2	1153	3	351.50	351.53	351.51	23	10	5072	1741
1154	7	1154	8	351.95	351.98	351.97	20	19	2717	2038
1156	1	1156	2	352.38	352.41	352.39	26	19	5745	3093
1157	5	1157	6	352.81	352.84	352.82	41	25	13589	4901
1158	9	1159	0	353.23	353.26	353.25	26	43	5749	7066
1160	7	1160	8	353.78	353.81	353.80	14	37	3110	6823
1161	7	1161	8	354.09	354.12	354.10	14	26	3230	5249
1162	7	1162	8	354.39	354.42	354.41	13	26	2227	3780
1163	7	1163	8	354.70	354.73	354.71	12	30	1730	3833
1164	6	1164	7	354.97	355.00	354.99	7	12	2541	4065
1165	5	1165	6	355.24	355.27	355.26	21	33	6004	7309
1166	4	1166	5	355.52	355.55	355.53	16	43	6789	15842
1167		1167	1	355.70	355.73	355.72	3	46	716	10845
1167	7	1167	8	355.91	355.95	355.93	2	39	459	8452
1168	3	1168	4	356.10	356.13	356.11	3	57	787	14719
1168	6	1168	7	356.19	356.22	356.20	3	43	632	7753
1168	9	1169		356.28	356.31	356.30	1	17	260	3119
1169	2	1169	3	356.37	356.40	356.39	4	15	736	2944
1169	4	1169	5	356.43	356.46	356.45	6	1	701	140
1170	1	1170	2	356.65	356.68	356.66	8	15	1801	3025
1170	2	1170	3	356.68	356.71	356.69	3	0	733	73
1170	4	1170	5	356.74	356.77	356.75	14	2	2539	282
1170	7	1170	8	356.83	356.86	356.84	18	1	3504	146

1171	1	1171	2	356.95	356.98	356.97	32	2	4914	218
1171	3	1171	4	357.01	357.04	357.03	35	0	8987	0
1171	6	1171	7	357.10	357.13	357.12	45	2	20275	531
1171	9	1172		357.20	357.23	357.21	48	0	10570	0
1172	2	1172	3	357.29	357.32	357.30	48	3	15568	512
1172	5	1172	6	357.38	357.41	357.39	34	1	6121	128
1172	8.5	1172	9	357.48	357.50	357.49	44	1	14559	199
1173	1	1173	2	357.56	357.59	357.58	52	2	8910	144
1173	4	1173	5	357.65	357.68	357.67	40	2	7641	196
1173	7	1173	8	357.74	357.77	357.76	5	2	439	135
1174		1174	1	357.84	357.87	357.85	4	1	416	104
1174	2	1174	3	357.90	357.93	357.91	2	1	205	164
1174	6	1174	7	358.02	358.05	358.03	0	0	0	0
1174	9	1175		358.11	358.14	358.12	0	1	55	110
1175	2	1175	3	358.20	358.23	358.22	0	0	28	28
1176	1	1176	2	358.48	358.51	358.49	2	0	170	0
1177	2	1177	3	358.81	358.84	358.83	0	0	0	0
1178	1	1178	2	359.08	359.12	359.10	0	0	114	114
1179	1	1179	2	359.39	359.42	359.40	0	0	0	56
1180	3	1180	4	359.76	359.79	359.77	2	0	337	0
1181	7	1181	8	360.18	360.21	360.20	6	0	747	53
1183	1	1183	2	360.61	360.64	360.62	10	1	1999	114
1184	5	1184	6	361.04	361.07	361.05	5	1	854	107
1185	9	1186		361.46	361.49	361.48	3	1	314	135
1186	7	1186	8	361.71	361.74	361.72	2	1	213	106
1188	1	1188	2	362.13	362.16	362.15	0	0	0	0
1189	5	1189	6	362.56	362.59	362.57	0	2	41	162
1191		1191	1	363.02	363.05	363.03	0	2	0	184
1192	8	1192	9	363.57	363.60	363.58	0	3	0	343
1194	3	1194	4	364.02	364.05	364.04	0	1	31	92
1195	7	1195	8	364.45	364.48	364.46	1	13	165	1705
1197	1	1197	2	364.88	364.91	364.89	9	3	2867	956
1198	6	1198	7	365.33	365.36	365.35	3	4	655	715
1200		1200	1	365.76	365.79	365.78	2	3	353	494
1201	4	1201	5	366.19	366.22	366.20	0	6	28	500
1202	4	1202	5	366.49	366.52	366.51	0	5	0	291
1203	8	1203	9	366.92	366.95	366.93	0	27	0	1593
1205	3.5	1205	4	367.39	367.41	367.40	0	18	0	1138
1206	7.5	1206	8	367.82	367.83	367.83	0	17	0	1513
1207	8	1207	9	368.14	368.17	368.15	0	13	26	819
1209	4	1209	5	368.63	368.66	368.64	0	12	0	831
1210	7.5	1210	8.5	369.04	369.07	369.05	0	7	0	570
1212	3	1212	4	369.51	369.54	369.52	0	3	0	307
1213	7	1213	8	369.94	369.97	369.95	0	1	140	279
1215	2	1215	3	370.39	370.42	370.41	0	1	0	271
1216	7	1216	8	370.85	370.88	370.87	0	0	0	111
1218	1	1218	2	371.28	371.31	371.29	0	0	0	82
1219	3	1219	4	371.64	371.67	371.66	0	0	0	126
1220	5	1220	6	372.01	372.04	372.02	0	0	0	45
1221	9	1222		372.44	372.47	372.45	0	1	0	126
1223	3	1223	4	372.86	372.89	372.88	0	0	0	0
1224	7	1224	8	373.29	373.32	373.30	0	0	0	36
1226	2	1226	3	373.75	373.78	373.76	0	4	0	443
1227	6	1227	7	374.17	374.20	374.19	0	9	0	633
1229		1229	1	374.60	374.63	374.61	0	1	0	131

Bass River TEX_{86} data											
top (feet)	top (tenth of feet)	bottom (feet)	bottom (tenth of feet)	top (mbs)	bottom (mbs)	Av depth (mbs)	TEX_{86}	T °C (Schouten et al 2002)	stdev	T °C (Schouten et al 2003)	stdev
1132	4	1132	5	345.16	345.19	345.17	0.80	34.6	0.3	30.2	0.1
1137	8	1137	9	346.80	346.83	346.82	0.69	27.3	0.3	26.1	0.2
1143	7	1143	8	348.60	348.63	348.62	0.74	30.7	0.1	28.0	0.1
1145	1	1145	2	349.03	349.06	349.04	0.81	35.6	0.4	30.7	0.2
1146	4	1146	5	349.42	349.45	349.44	0.83	36.4	0.2	31.2	0.1
1147	7	1147	8	349.82	349.85	349.83	0.82	36.0	0.0	30.9	0.0
1149	1	1149	2	350.25	350.28	350.26	0.84	37.4	0.4	31.8	0.2
1153	2	1153	3	351.50	351.53	351.51	0.85	38.1	0.2	32.1	0.1
1158	9	1159	0	353.23	353.26	353.25	0.86	38.4	0.3	32.3	0.2
1160	7	1160	8	353.78	353.81	353.80	0.87	39.0	0.3	32.6	0.2
1162	7	1162	8	354.39	354.42	354.41	0.87	39.3	1.1	32.8	0.6
1163	7	1163	8	354.70	354.73	354.71	0.87	39.6	0.4	33.0	0.2
1164	6	1164	7	354.97	355.00	354.99	0.89	41.0	0.3	33.7	0.2
1165	5	1165	6	355.24	355.27	355.26	0.89	40.7	0.3	33.6	0.2
1166	4	1166	5	355.52	355.55	355.53	0.88	40.4	0.6	33.4	0.3
1168	3	1168	4	356.10	356.13	356.11	0.89	40.8	0.4	33.6	0.2
1168	6	1168	7	356.19	356.22	356.20	0.89	41.0	0.2	33.7	0.1
1169	2	1169	3	356.37	356.40	356.39	0.91	41.9	0.6	34.3	0.3
1169	4	1169	5	356.43	356.46	356.45	0.91	41.9	0.3	34.2	0.2
1170	1	1170	2	356.65	356.68	356.66	0.89	40.7	0.5	33.6	0.3
1170	2	1170	3	356.68	356.71	356.69	0.90	41.5	0.4	34.0	0.2
1170	4	1170	5	356.74	356.77	356.75	0.90	41.3	0.4	33.9	0.2
1170	7	1170	8	356.83	356.86	356.84	0.90	41.3	0.5	33.9	0.3
1171	1	1171	2	356.95	356.98	356.97	0.92	42.6	0.4	34.6	0.2
1171	3	1171	4	357.01	357.04	357.03	0.91	42.2	0.4	34.4	0.2
1171	6	1171	7	357.10	357.13	357.12	0.87	39.2	0.4	32.7	0.2
1171	9	1172		357.20	357.23	357.21	0.87	39.5	0.7	32.9	0.4
1172	2	1172	3	357.29	357.32	357.30	0.85	38.2	0.4	32.2	0.2
1172	5	1172	6	357.38	357.41	357.39	0.80	35.0	0.2	30.4	0.1
1172	8.5	1172	9	357.48	357.50	357.49	0.78	33.2	0.0	29.4	0.0
1173	1	1173	2	357.56	357.59	357.58	0.76	31.7	0.1	28.6	0.0
1173	4	1173	5	357.65	357.68	357.67	0.76	32.0	0.0	28.7	0.0
1174		1174	1	357.84	357.87	357.85	0.77	32.4	0.1	28.9	0.0
1174	2	1174	3	357.90	357.93	357.91	0.77	32.8	0.1	29.2	0.1
1174	6	1174	7	358.02	358.05	358.03	0.77	32.6	0.2	29.1	0.1
1175	2	1175	3	358.20	358.23	358.22	0.75	31.6	0.0	28.5	0.0
1176	1	1176	2	358.48	358.51	358.49	0.75	31.1	0.2	28.2	0.1
1177	2	1177	3	358.81	358.84	358.83	0.73	30.0	0.1	27.6	0.1
1179	1	1179	2	359.39	359.42	359.40	0.73	29.9	0.0	27.6	0.0
1180	3	1180	4	359.76	359.79	359.77	0.73	30.3	0.6	27.8	0.3
1184	5	1184	6	361.04	361.07	361.05	0.77	32.6	0.1	29.1	0.1
1189	5	1189	6	362.56	362.59	362.57	0.71	28.6	0.0	26.8	0.0
1195	7	1195	8	364.45	364.48	364.46	0.74	30.9	3.0	28.1	1.7
1196	4	1196	5	364.66	364.69	364.68	0.74	30.4	0.1	27.9	0.1
1201	4	1201	5	366.19	366.22	366.20	0.74	30.5	0.2	27.9	0.1

Bass River Dinocyst $\delta^{13}C$ data									
top (feet)	top (tenth of feet)	bottom (feet)	bottom (tenth of feet)	top (mbs)	bottom (mbs)	Depth (mbs)	Dinocyst $\delta^{13}C$	stdev
1150	4	1150	5	350.64	350.67	350.66	-26.67	
1154	7	1154	8	351.95	351.98	351.97	-26.64	
1158	9	1159	0	353.23	353.26	353.25	-27.49	
1161	7	1161	8	354.09	354.12	354.10	-27.66	
1165	5	1165	6	355.24	355.27	355.26	-28.09	0.13
1167		1167	1	355.70	355.73	355.72	-27.43	
1168	3	1168	4	356.10	356.13	356.11	-28.14	
1168	6	1168	7	356.19	356.22	356.20	-28.30	
1168	9	1169		356.28	356.31	356.30	-27.64	
1169	2	1169	3	356.37	356.40	356.39	-28.26	
1169	4	1169	5	356.43	356.46	356.45	-27.63	0.05
1170	1	1170	2	356.65	356.68	356.66	-28.14	
1170	2	1170	3	356.68	356.71	356.69	-28.52	
1170	4	1170	5	356.74	356.77	356.75	-28.80	
1170	7	1170	8	356.83	356.86	356.84	-28.12	
1171	1	1171	2	356.95	356.98	356.97	-28.45	0.52
1171	3	1171	4	357.01	357.04	357.03	-27.79	0.13
1171	6	1171	7	357.10	357.13	357.12	-25.73	0.18
1171	9	1172		357.20	357.23	357.21	-25.61	0.08
1172	2	1172	3	357.29	357.32	357.30	-25.27	0.06
1172	5	1172	6	357.38	357.41	357.39	-24.24	0.06
1172	8.5	1172	9	357.48	357.50	357.49	-24.16	0.06
1173	1	1173	2	357.56	357.59	357.58	-23.84	
1173	4	1173	5	357.65	357.68	357.67	-23.80	
1173	7	1173	8	357.74	357.77	357.76	-24.21	0.21
1174		1174	1	357.84	357.87	357.85	-24.10	
1174	2	1174	3	357.90	357.93	357.91	-23.76	
1174	6	1174	7	358.02	358.05	358.03	-23.81	
1174	9	1175		358.11	358.14	358.12	-24.04	
1176	1	1176	2	358.48	358.51	358.49	-23.86	
1178	1	1178	2	359.08	359.12	359.10	-21.62	0.19
1180	3	1180	4	359.76	359.79	359.77	-23.00	0.19
1183	1	1183	2	360.61	360.64	360.62	-22.61	

Table 1b. Wilson Lake

Wilson Lake *Apectodinium* data		
Depth (ft)	Depth (m)	% *Apectodinium*
300.23	91.51	14
302.60	92.23	2
304.95	92.95	0
306.50	93.42	1
307.84	93.83	0
309.72	94.40	1
311.00	94.79	3
313.13	95.44	35
314.82	95.96	25
318.05	96.94	46
319.75	97.46	46
321.16	97.89	4
322.84	98.40	3
324.47	98.90	4
326.21	99.43	5
327.85	99.93	8
330.44	100.72	4
332.11	101.23	4
333.75	101.73	8
335.27	102.19	3
336.85	102.67	14
338.40	103.14	4
339.97	103.62	5
341.45	104.07	2
343.10	104.58	6
344.63	105.04	7
346.17	105.51	8
347.80	106.01	11
350.70	106.89	19
352.37	107.40	14
352.70	107.50	15
354.00	107.90	6
355.23	108.27	22
356.26	108.59	33
356.60	108.69	55
356.92	108.79	30
357.24	108.89	31
357.54	108.98	25
357.75	109.04	35
358.70	109.33	43
359.00	109.42	51
359.50	109.58	32
360.12	109.76	42
360.25	109.80	41
360.65	109.93	53
361.05	110.05	40
361.10	110.06	42
361.15	110.08	33
361.35	110.14	40
361.43	110.16	38
361.45	110.17	49
361.70	110.25	37

362.00	110.34	31
362.25	110.41	26
362.65	110.54	4
362.90	110.61	0
363.25	110.72	0
363.30	110.73	0
363.55	110.81	1
363.95	110.93	2
364.15	110.99	0
364.50	111.10	0
364.85	111.21	0
365.35	111.36	0
365.85	111.51	4
366.20	111.62	3
366.85	111.82	1
367.35	111.97	0
367.85	112.12	0
368.50	112.32	0
369.10	112.50	0
369.40	112.59	0
369.95	112.76	0

Wilson Lake TEX_{86} data

Depth (ft)	Depth (m)	TEX_{86}	T °C (Schouten et al 2003)	T °C (Schouten et al 2003)	reference (for previously published data)
300.23	91.51	0.79	34.1	29.9	from Zachos et al., 2006
304.95	92.95	0.74	31.0	28.2	from Zachos et al., 2006
307.84	93.83	0.77	32.3	28.9	from Zachos et al., 2006
314.82	95.96	0.70	28.2	26.6	from Zachos et al., 2006
318.05	96.94	0.87	39.3	32.8	from Zachos et al., 2006
321.16	97.89	0.87	39.6	33.0	from Zachos et al., 2006
324.47	98.90	0.89	40.8	33.6	from Zachos et al., 2006
327.85	99.93	0.89	40.4	33.4	from Zachos et al., 2006
332.11	101.23	0.89	40.5	33.5	from Zachos et al., 2006
338.40	103.14	0.91	42.1	34.3	from Zachos et al., 2006
343.10	104.58	0.89	41.0	33.7	from Zachos et al., 2006
346.17	105.51	0.86	38.4	32.3	from Zachos et al., 2006
350.42	106.81	0.88	40.2	33.3	from Zachos et al., 2006
354.00	107.90	0.93	43.4	35.1	from Zachos et al., 2006
355.25	108.28	0.92	42.6	34.7	
356.35	108.62	0.91	41.8	34.2	
356.75	108.74	0.91	41.9	34.2	
357.35	108.92	0.91	41.7	34.1	
357.75	109.04	0.89	40.9	33.7	
358.75	109.35	0.86	38.4	32.3	
359.05	109.44	0.85	38.2	32.2	
360.10	109.76	0.78	33.4	29.5	from Zachos et al., 2006
360.25	109.80	0.84	37.2	31.6	
360.65	109.93	0.78	33.3	29.5	
361.05	110.05	0.73	29.9	27.6	
361.15	110.08	0.76	31.7	28.6	
361.35	110.14	0.72	29.5	27.3	
361.45	110.17	0.71	28.7	26.9	
361.71	110.25	0.70	28.0	26.5	from Zachos et al., 2006
361.75	110.26	0.70	28.2	26.6	
362.05	110.35	0.69	27.4	26.2	
362.25	110.41	0.71	28.4	26.7	
362.65	110.54	0.71	28.3	26.7	
362.95	110.63	0.70	28.2	26.6	
363.25	110.72	0.71	28.5	26.8	
363.29	110.73	0.66	25.2	25.0	from Zachos et al., 2006
363.55	110.81	0.68	26.4	25.6	
363.95	110.93	0.70	28.2	26.6	
364.55	111.11	0.70	28.1	26.6	
364.85	111.21	0.69	27.7	26.3	
365.41	111.38	0.70	28.0	26.5	
365.49	111.40	0.72	29.3	27.3	from Zachos et al., 2006
365.88	111.52	0.70	28.2	26.6	
366.18	111.61	0.70	28.3	26.7	
366.85	111.82	0.71	28.9	27.0	
367.38	111.98	0.71	28.9	27.0	
367.82	112.11	0.73	29.8	27.5	from Zachos et al., 2006
368.53	112.33	0.71	28.9	27.0	
369.10	112.50	0.71	28.6	26.9	
369.39	112.59	0.70	27.9	26.5	from Zachos et al., 2006
369.65	112.67	0.69	27.1	26.0	
370.00	112.78	0.68	26.6	25.7	

Wilson Lake Dinocyst $\delta^{13}C$ data			
Depth (ft)	Depth (m)	Dinocyst $\delta^{13}C$	stdev
307.84	93.83	-22.96	
311.00	94.79	-25.19	
314.82	95.96	-24.67	
319.75	97.46	-26.82	
326.21	99.43	-27.16	
327.85	99.93	-27.61	
330.44	100.72	-26.69	
333.75	101.73	-27.45	
336.85	102.67	-26.91	
339.97	103.62	-26.87	
352.37	107.40	-27.89	
352.70	107.50	-27.87	0.12
354.00	107.90	-27.72	
355.23	108.27	-27.77	
356.26	108.59	-27.64	
356.60	108.69	-27.70	
356.92	108.79	-26.62	
357.24	108.89	-27.36	
357.54	108.98	-26.89	
357.75	109.04	-26.29	
358.70	109.33	-26.19	
359.00	109.42	-25.99	
359.50	109.58	-25.85	
360.12	109.76	-25.31	
360.25	109.80	-25.46	0.15
360.65	109.93	-24.39	0.12
361.05	110.05	-23.13	0.16
361.10	110.06	-22.56	
361.15	110.08	-23.02	
361.35	110.14	-24.37	
361.43	110.16	-23.48	
361.45	110.17	-23.44	0.03
361.70	110.25	-22.45	0.24
362.00	110.34	-23.85	
362.25	110.41	-23.33	
362.65	110.54	-23.07	0.09
362.90	110.61	-20.82	0.24
363.25	110.72	-21.55	
363.30	110.73	-20.89	0.08
363.55	110.81	-21.69	
363.95	110.93	-22.49	
364.15	110.99	-22.35	
364.50	111.10	-22.09	0.06
364.85	111.21	-22.94	
365.35	111.36	-23.82	
365.85	111.51	-23.18	
366.20	111.62	-23.25	
366.85	111.82	-22.80	
367.35	111.97	-23.34	
367.85	112.12	-22.84	0.02
368.50	112.32	-23.28	
369.10	112.50	-21.64	
369.40	112.59	-21.17	
369.95	112.76	-19.96	

Table 1c. North Sea FINA Well 30/14-1

North Sea *Apectodinium* data			
feet	inch	Depth (mbsf)	% *Apectodinium*
9425	4	2872.84	0
9445	0	2878.84	0
9452	6	2881.12	1
9465	0	2884.93	5
9485	0	2891.03	0
9505	0	2897.12	52
9525	0	2903.22	31
9532	6	2905.51	62
9545	0	2909.32	39
9555	0	2912.36	41
9565	0	2915.41	68
9579	0	2919.68	59
9587	0	2922.12	65
9595	0	2924.56	57
9603	0	2926.99	35
9604	0	2927.30	16
9606	0	2927.91	0
9608	0	2928.52	0
9610	0	2929.13	0
9627	6	2934.46	0
9642	6	2939.03	0

North Sea δ^{13}C TOC			
feet	inch	Depth (mbsf)	δ^{13}C TOC
9465		2884.93	-26.89
9505		2897.12	-29.16
9525		2903.22	-28.62
9552	6	2911.60	-31.21
9555		2912.36	-31.68
9557	6	2913.13	-31.73
9560		2913.89	-31.49
9562	6	2914.65	-30.53
9565		2915.41	-31.79
9565	2	2915.46	-31.26
9567	6	2916.17	-32.11
9570		2916.94	-31.76
9572	6	2917.70	-30.56
9575		2918.46	-31.70
9576		2918.76	-31.45
9577		2919.07	-28.28
9579		2919.68	-29.57
9581		2920.29	-29.63
9583		2920.90	-28.58
9587		2922.12	-29.76
9589		2922.73	-29.59
9591		2923.34	-28.92
9593		2923.95	-29.13
9595		2924.56	-28.25
9597		2925.17	-28.38
9599		2925.78	-27.28
9601		2926.38	-26.67
9603		2926.99	-26.11
9604		2927.30	-26.25
9606		2927.91	-26.09
9608		2928.52	-26.33
9610		2929.13	-26.31
9642	6	2939.03	-25.44